Structural and Mechanical Heterogeneity of the Erythrocyte Membrane Reveals Hallmarks of Membrane Stability

Laura Picas[a], *Félix Rico*[a], *Maxime Deforet*[b], *Simon Scheuring*[a,*]

[a]U1006 INSERM, Aix-Marseille Université, Parc Scientifique de Luminy, Marseille, F-13009 France

[b]PhysicalChemistry Curie - Institut Curie / CNRS UMR 168 / Paris, France.

[*]Corresponding author. Simon Scheuring. Parc Scientifique et Technologique de Luminy, Bâtiment Inserm TPR2 bloc 5, 163 avenue de Luminy, 13009 Marseille (France). Telephone number : +33 (0)4 91 82 87 77. simon.scheuring@inserm.fr

Atomic Force Microscopy, mechanics, erythrocyte, spectrin.

Abstract

The erythrocyte membrane, a metabolically regulated active structure that comprises lipid molecules, junctional complexes and the spectrin network, enables the cell to undergo large passive deformations when passing through the microvascular system. Here we use atomic force microscopy (AFM) imaging and quantitative mechanical mapping at nanometer resolution to correlate structure and mechanics of key components of the erythrocyte membrane, crucial for cell integrity and function. Our data reveals structural and mechanical heterogeneity modulated by the metabolic state at unprecedented nanometer resolution. ATP-depletion, reducing skeletal junction phosphorylation in RBC cells, leads to membrane stiffening. Analysis of ghosts and shear-force opened erythrocytes show that, in absence of cytosolic kinases, spectrin phosporylation results in membrane stiffening at the extracellular face and a reduced junction remodeling in response to loading forces. Topography and mechanical mapping of single components at the cytoplasmic face reveals that, surprisingly, spectrin phosphorylation by ATP softens individual filaments. Our findings suggest that, besides the mechanical signature of each component, the RBC membrane mechanics is regulated by the metabolic state and the assembly of its structural elements.

An essential feature of red blood cells (RBCs) relies on their capability to undergo large passive deformations throughout narrow capillaries of the microvasculature during their 120-days life span. Mature erythrocytes are non-nucleated, and their structural integrity depends on the particular attributes of the plasma membrane in terms of antigenic and transport activity but importantly, on its remarkable mechanical properties.[1] Many studies have unraveled the complexity hidden in the exceptional properties of the erythrocyte plasma membrane thanks to the development of isolation methods and techniques for the biochemical, structural and functional characterization of the diverse components that integrate the erythrocyte membrane. [1-5] The RBC membrane consists of an α and β-spectrin lattice that is linked to the lipid bilayer thought membrane proteins, most of them integrating multiprotein complexes. The most abundant membrane proteins are band 3, aquaporin-1, glycophorin A and C and the rhesus proteins, Rh and RhAG. Key for the structural integrity of the membrane are two macromolecular complexes: the ankyrin-based complex, which is thought to work as a metabolon, and the 4.1R complex that integrates the main components of the skeleton network junctions, *i.e*. spectrin, actin and protein 4.1R, together with other proteins (adducin, tropomysoin, topomodulin, p55, and demantin) and membrane proteins such as glycophorin C (GPC) or band 3 (for a review see, [1]).

It is well established, that far from being static, the RBC membrane is a metabolically regulated active structure.[5] Thus, a number of works have shown the regulatory mechanism of Ca^{2+}, phosphatidylinositol 4,5-bisphosphate (PIP_2) or protein phosphorylation on the membrane. As a result, posttranslational modifications of proteins integrating the skeleton network junctions are known to induce specific changes in the membrane mechanical function. [6, 7]

In a significant effort to join the gap between biochemistry and physical properties, several biophysical studies of the erythrocyte membrane mechanics have revealed the underlying complexity of a dynamic structure that involves the cooperative assembly and disassembly of protein complexes and the spectrin network.[3] However, direct visualization of the structure, functionality and mechanics of the components involved in the RBC membrane architecture is yet in its earliest attempts.[8-10] Among the emerging techniques capable to provide information down to the nanoscale, atomic force microscopy [11] promises breakthrough capabilities as a versatile tool to reveal cell architecture, simultaneously providing structural information from topographical and mechanical properties through force spectroscopy maps.[12]

In this work, we implemented a recently developed AFM-based technique, the PeakForce Quantitative Nanomechanical Mapping (PF-QNM [13]), to assess the structure and mechanics of the erythrocyte membrane by providing concomitant topography imaging and quantitative mechanical mapping at an unprecedented nanometer resolution. The combination of topography and mechanical maps at physiological conditions, allowed us to correlate structure and function under different metabolic states at the sub-cellular level. The aim of this study was to determine the mechanical role of the structural components of the erythrocyte membrane and the effect of protein phosphorylation at molecular level. PF-QNM analysis of junctional complexes and the spectrin network proves that the RBC membrane displays high mechanical heterogeneity of components. Our results show that β-spectrin phosphorylation plays a key role in the erythrocyte membrane stability by modulating its compliance and enhancing the maintenance of stable network interactions.

Results

The study presented here takes advantage of an extensive bibliography reporting methods to access both sides of the RBC plasma membrane.[2, 14, 15] Moreover, several publications cover preparative methods to study intact RBC, ghosts and shear-force opened erythocytes to get access to decipher the structural properties of the extracellular and cytoplasmic faces of the RBC membrane.[2, 8, 15] In this work three preparation methods of erythrocytes were used to gather in-depth characterization of their topographical and mechanical features under physiological conditions. The feasibility of these preparations for AFM studies (including intact RBC, ghosts and shear-force opened RBC exposing the cytoplasmic face) was first confirmed through optical microscopy, where both membrane and F-actin were stained (Supporting Figure S1).

ATP-depletion induces membrane stiffening on intact RBCs

We first evaluated the capabilities of the PF-QNM technique in detecting mechanical differences on intact RBC (ATP-depleted and ATP-containing erythrocytes) directly immobilized on poly-L-lysine (PLL) coated mica (Figure 1). We found that, whereas topographic features did not report significant structural changes at the level of the RBC membrane, significant variations of the elastic modulus were readily detected when comparing ATP-containing and ATP-depleted erythrocytes at low loading forces (*i.e.* 300 pN). Profile analysis extracted from elasticity maps reported that ATP depletion promotes stiffening of the RBC membrane without compromising cell thickness (see Supporting Figures S2 and S3). Evaluation of the RBC membrane response upon increasing applied loading force (350 pN, 400 pN, 450 pN, and 500 pN) showed gradual stiffening of intact RBC as a function of force and depending on the absence or presence of ATP

(Supporting Figures S2 and S3). After applying 500 pN, initial values of elastic modulus and deformation were recovered when retrieving to the initial load of 300 pN.

Structural and mechanical heterogeneity of the RBC plasma membrane

Direct evaluation of the sub-cellular organization of the RBC membrane was performed through PF-QNM imaging and mechanical characterization of both cytoplasmic and extracellular faces under physiological conditions and at high resolution. Considering the fact that the glycocalyx might hamper detection of fine topographic features on the extracellular face and that the cytoplasmic membrane face is expected to be rather crowded with membrane skeleton elements,[16] inspection of both sides of the RBC plasma membrane turns essential for a full characterization. To accomplish this, observations of the extracellular side were performed by imaging ghosts obtained from immobilized RBCs on PLL coated mica, whereas the cytoplasmic face was accessed after shear stress opening of immobilized erythrocytes on PLL coated mica and subsequent spectrin removal (Figure 2 and Supporting Figure S1). Analysis of the erythrocyte membrane from topographic images (Figure 2A) provided evidences of readily detectable protrusions separated by an average distance of 200 nm, on both sides of the plasma membrane, correlating with the expected sub-cellular organization of skeleton junctions.[17] Certainly, the fact that membrane skeleton junctions are rather preserved all through the plasma membrane, even after spectrin removal, confirms their functionality as underpinning of the skeleton network. Evaluation of the mechanical properties on both sides of the erythrocyte membrane was assessed from the corresponding elasticity and deformation maps. Interestingly, analysis of these images showed that skeleton junctions are stiffer and less deformable than any other structure of the plasma membrane.

MgATP stiffens the extracellular face of the RBC plasma membrane and restrains lateral protein interactions

In order to assess the influence of the metabolic state on the physical properties of the erythrocyte membrane, we analyzed the topographical and mechanical features of the extracellular face through imaging of immobilized ghosts at different loading forces, before and after MgATP addition. It is well established that addition of MgATP in ghosts results in protein phosphorylation without affecting ATPase activity.[7] Topographical images acquired before and after addition of MgATP are displayed in Figure 3A, together with the corresponding elasticity and deformation maps obtained at 300 pN loading force. Better tracking of the skeleton components beneath the glycocalix and plasma membrane was performed through morpho-mathematical image processing [18] of topography images and subsequent skeleton extraction and overlay with elasticity and deformation maps. The topographical features of the extracellular membrane display a large number of protruding structures connected through an underlying mesh (Figure 3A). In terms of RBC membrane structure, the distribution of lumps, separated by an average distance of 205 ± 15 nm, corresponds to the expected lateral distribution of skeleton junctions.[17] Average distance between protrusions was obtained by pair correlation function analysis of the topography images acquired on the extracellular membrane face. Nevertheless, the tip interaction with the oligosaccharide chains of the glycocalix might explain a decrease in the lateral resolution (> 15-20 nm) of topographical features detected, without necessarily affect the mechanical response.[19]

The topographical features of the extracellular side of RBC membrane did not substantially change before and after MgATP addition (Figure 3A). However, evaluation of the elasticity and

deformation maps showed significant changes of the membrane mechanics after protein phosphorylation, as documented in the elastic modulus and deformation graphs (Figures 3B and 3C). Skeleton map extractions from topography images were analyzed to assign mechanical properties to the structural components of the RBC membrane and skeleton network. Thus, inspection of the entire elasticity and deformation maps at 300 pN revealed that network junctions were stiffer and less deformable than the overall membrane mechanics (Figure 2). MgATP inclusion and subsequent protein phosphorylation triggered changes in the elastic modulus and deformation, especially at the network junctions. Indeed, MgATP addition promoted a clear stiffening of the membrane components.

Studying an experimental range of loading forces (350 pN, 400 pN, 450 pN, and 500 pN) and before and after MgATP-mediated phosphorylation, revealed a general trend for increased elastic modulus and deformation of the extracellular face of the RBC membrane (graphs in Supporting Figure S4). Importantly, upon second investigation at the initial 300 pN loading force, the membrane mechanics recovered elastic modulus and deformation values, proving the reversibility of the process and the elastic properties of the plasma membrane (Supporting Figure S5).

In depth characterization of membrane remodeling triggered by MgATP addition was evaluated from AFM topography images and skeleton pattern extraction at the extracellular face of the RBC membrane. Thus, tracking of the lateral reorganization of skeleton junctions upon increasing loading forces was performed before and after protein phosphorylation (Figure 4 and Supporting Figure S6 for raw data). Quantification of skeleton junctions remodeling was performed by using as reference sample the network pattern and skeleton components lattice as assessed at 300 pN loading force (Figure 4, *purple*), and tracking the lateral reorganization (junctions displacements ≥ 50 nm) (Figure 4, *orange*). As observed from graphs in Figure 4, the

trend of skeleton junctions remodeling progressively increased upon applying higher loading forces in absence of MgATP thus, suggesting a discrete rearrangement of membrane components in response to external forces. Lateral fluctuations of skeleton junctions were of the order of tens of nanometers, irrespective of their apparent size. Interestingly, protein phosphorylation triggered by MgATP inclusion yielded a complete inhibition of membrane components rearrangement at any of the studied forces (Figure 4).

MgATP softens the cytoplasmic face of RBC plasma membrane through spectrin phosphorylation

Analogously, in depth characterization of the structural and mechanical features of the cytoplasmic face of the erythrocyte membrane was performed before and after MgATP addition. In this case, shear-force opened RBCs exposing the spectrin network and cytoplasmic components of the RBC membrane were prepared. Importantly, absence of glycocalix enabled a more detailed characterization of the membrane structure and improved spectrin skeleton map extraction (Figure 5A). Inspection of AFM topography images showed a lattice of network junctions separated by an average distance of 137 ± 10 nm and interconnected through a mesh-like structure, irrespective of MgATP addition, as assessed by pair correlation function analysis.

As we already observed for the extracellular face, the topographic features reporting the structural organization of the cytoplasmic side were not affected by MgATP-mediated protein phosphorylation. However, evaluation of elasticity and deformation maps at the lowest loading force assessed (300 pN) revealed indeed significant changes in the mechanical heterogeneity of the cytoplasmic face after MgATP addition. As observed in Figure 5A, MgATP inclusion substantially decreased the cytoplasmic membrane elasticity modulus. Complete analysis of the overall set of loading forces studied (350 pN, 400 pN, 450 pN, and 500 pN) revealed a trend of

elastic modulus and deformation similar to that already reported for the extracellular side and a retrieving of initial elastic modulus at 300 pN (Supporting Figure S7). Further characterization of MgATP phosphorylation and alteration of skeleton components, in particular the spectrin lattice, was determined on shear-force opened RBCs with either intact or removed spectrin network in absence or presence of MgATP (Figure 6). PF-QNM analysis of these two samples reported readily detectable topographic differences, where spectrin removal from the cytopasmic face resulted in a strongly corrugated membrane surface without spectrin-junction interconnections. In terms of topography, MgATP addition did not modify the apparent topographical features for any of the studied samples. In contrast, further analysis of elasticity maps evidenced substantial mechanical changes depending on MgATP addition only for those preparations where the spectrin network was preserved. Indeed, thorough inspection of spectrin containing samples showed that changes in elastic modulus especially occurred in structures assigned to the spectrin lattice. Absence of cytosolic kinases favors phosphorylation of β-spectrin by a membrane-bound kinase, casein kinase I.[7] Thus, phosphorylation of β-spectrin results in a notable decrease of the elastic modulus of individual filaments.

Discussion

In this work we have examined the structure and mechanics of key components of the RBC plasma membrane, the spectrin lattice and network junctions. Our work revealed unprecedented resolution of the RBC membrane and proves the heterogeneity of the erythrocyte membrane in terms of structural components and importantly, of their mechanical properties. Evaluation of intact RBC and both sides of the erythrocyte membrane showed that whereas topography images

did not report particular structural modifications upon protein phosphorylation, important changes at the mechanical level took place.

Our results obtained on intact RBC (Figure 1) validated the capabilities of the PF-QNM technique to detect mechanical changes at the sub-cellular level and allowing correlation to structural features. The measurements performed on intact erythrocytes (Figure 1) showed that intracellular ATP increases the compliance of the membrane, as has been shown through fluctuation analysis.[4, 20] It is, however, in disagreement with mechanical measurements using optical tweezers.[21] This disagreement may be due to the different strains at which mechanics were probed. While Yoon and coworkers applied large deformation to the whole RBC and measured related changes of the cell shape upon stretching, our data displays the mechanical properties upon small compression of subcellular components that might behave differently. Our data reported that ATP-depletion results in a stiffer membrane, possibly as a consequence of the increased number of spectrin-membrane connections that anchors the bilayer more frequently, stabilizing it. Thus, release of junctional network interconnections in ATP-activated cells will lead to a decrease in membrane elasticity whereas in the opposite case, ATP-depletion mediates spectrin-membrane connections and the consequent membrane stiffening as observed in Figure 1.

Under normal conditions, phosphorylation of 4.1R by PKC appears to trigger the relaxation of the erythrocyte membrane through loosening of the link between the spectrin network and the lipid membrane *via* the 4.1R complex, favoring the cell to undergo large deformations without compromising its integrity (Figure 7, *intact erythrocytes*). Importantly, this phenomenon is reversible and takes place while the spectrin network is still linked to the membrane, mostly through spectrin-ankyrin interactions.[3]

It is clear that posttranslational modifications, such as phosphorylation, directly modulate the mechanical stability of the RBC plasma membrane. However, the complexity of this response relies on the fact that a number of skeleton components, with exception of actin, are phosphoproteins and therefore, susceptible to cytosolic kinases and phosphatases.[5,6] Besides the effect of 4.1R phosphorylation in modulating the functional interactions within the 4.1R complex, early studies reported that membrane stability is also fine regulated by β-spectrin phosphorylation through the membrane-bound casein kinase I.[7]

Topographic and mechanical images displayed in Figure 2 reveal the complexity and heterogeneity of the structural components that integrate the erythrocyte plasma membrane (see Supporting Figure S4 for structural details on intact RBCs). Indeed, network junctions can be readily identified by the lumps observed at both cytoplasmic and extracellular sides of the RBC membrane, separated by an average distance of 137 nm and 200 nm, respectively, that coincides with the expected 200 nm estimated by other works.[17] The shorter average distance found at the cytoplasmic side might be due to the improved resolution achieved at this face, allowing us to detect smaller skeleton junctions and therefore, lower average distances. Importantly, the fact that these structures appear at both sides of the RBC membrane stiffer and less deformable than other structural components might be a hint of their possible mechanical role. This observation suggests that besides being a structural sustain and anchoring the spectrin lattice, skeleton junctions might operate as mechanically stable regions throughout the RBC membrane.

Evaluation of the topography and mechanical response of RBC membrane components at the extracellular and cytoplasmic face reported evidences of the effect of MgATP as a modulator of membrane stability through the different metabolic states of the spectrin network. Interestingly, the cytoplasmic face was about one order of magnitude stiffer than the extracellular face. This

difference might be due to the glycocalyx on the extracellular face and, to some extent, the direct probing of the membrane skeleton components on the cytoplasmic face and not the overall membrane mechanical response. More importantly, the higher elastic modulus of the cytoplasmic components reflects that our measurements probe the actual elasticity of the isolated components themselves, independently of the more complex response of the overall membrane probed on the extracellular face.

The absence of cytosolic kinases in ghosts favors phosphorylation of β-spectrin by membrane-bound casein kinase I.[7] Specifically, MgATP mediates the phosphorylation of serine residues near the C-terminus of β-spectrin.[7] Indeed, changes induced after spectrin phoshporylation are involved in membrane destabilization and cell deformation in hereditary elliptocytosis.[22]

Inspection of elasticity and deformation maps at the extracellular face of ghosts showed that spectrin phosphorylation triggered membrane stiffening (Figure 3). Moreover, tracking of lateral remodeling of skeleton junctions evidenced that spectrin phosphorylation restricts lateral rearrangement of membrane components in response to external forces (Figure 4). These observations confirm the role of spectrin phosphorylation in modulating RBC membrane stability.[7] Certainly, specific β-spectrin phosphorylation is capable to alter membrane mechanics by enhancing the spectrin network anchoring as reflected by a rise in the membrane stiffening and lower lateral mobility of the RBC membrane components. These finding was equally confirmed after evaluation of samples facing different scenarios of the cytoplasmic membrane, *i.e.* in presence and absence of spectrin network, showing the selectivity of MgATP in mediating the phosphorylation of spectrin in absence of cytosolic kinases (Figure 5). Notably, spectrin phoshporylation is materialized in a clear decrease in the elastic modulus of spectrin filaments

and no apparent rearrangement of the spectrin lattice within the skeleton junctions (Supporting Figure S8).

Our studies on ghosts suggest that massive phosphorylation of spectrin could improve the skeleton anchoring either by increasing the spectrin-ankyrin affinity or by the stabilization of spectrin tetramers (Figure 7, *ghosts*). If the latter were true, we would expect stiffer spectrin filaments upon phosphorylation. Since we observe the opposite effect, we conclude that a more compliant spectrin after phosphorylation is more prone to deform and form contacts with ankyrin, than a non-phosphorylated, rigid spectrin. The possibility of α, β-spectrin head-to-head dissociation and spectrin domain unfolding was previously reported to illustrate the observed fluctuations of F-actin protofilaments.[23] However, under our experimental conditions, no important spectrin remodeling was observed after phosphorylation (Supporting Figure S7), suggesting that the main mechanical response should be attributed to the modulation of the spectrin-ankyrin interaction. Indeed, this situation might describe the stiffening of the extracellular face after MgATP addition, and why a progressive increase of the loading force did not induce lateral dislocation of network junctions. Thus, in absence of MgATP, a stiffer spectrin filament and a weaker spectrin-ankyrin interaction might explain the discrete remodeling of skeleton junctions reported upon increasing loading forces in Figure 4.

To conclude, we have mapped the supramolecular organization and mechano-functional state of individual components of the RBC membrane at unprecedented nanometer resolution. We detected mechanically stable membrane skeleton junctions that confirm their role as underpinning elements of the skeleton network, while flexible spectrin filaments allowing network reorganization. Our observations suggest that modulation of the mechanical stability of the RBC membrane by ATP is mainly governed by the interaction between the different skeletal

components and not directly by modulation of the mechanical properties of the components themselves. During large deformations experienced by the RBC on narrow capillaries, membrane integrity is assured by ATP-induced phosphorylation of 4.1R, which increases membrane compliance by loosening the spectrin-lipid interaction. The observed decrease in spectrin stiffness upon phosphorylation may allow formation of many junctions allowing fast, reversible rearrangement of the spectrin network upon large deformations, thus indirectly modulating the mechanical stability of the membrane (Figure 7). Importantly, we show that changes in spectrin biochemistry not detected in terms of structure can be mechanically identified. As a consequence, modulation of the mechanical properties of membrane components at the single-molecule level might be a hallmark of the erythrocyte membrane stability and thus, a hint in detecting structural failures as a consequence of pathologies that might affect protein linkages (eg. hereditary elliptocytosis or hereditary pyrpoikilocytosis) or even upon massive phosphorylation after invasion of protozoa *Plasmodium falciparum* during malaria infection.

Materials and Methods

Red blood cell preparations

First, coated supports were obtained by deposition of a 0.01% poly-L-lysine (PLL) suspension on freshly cleaved mica. This suspension was kept 24h at 4ºC to allow homogeneous coating, excess of PLL was washed by rinsing ten times with milliQ water. Previous to each preparation, coated supports were equilibrated with fresh PBS, 0.2 mM EDTA buffer (salt buffer, SB) and checked with the AFM to assure a uniform PLL coating.

Human venous blood was collected from healthy donors after informed consent. Cells were first washed by centrifuging three times at 1500*g* for 10 min in fresh PBS, pH 7.4, 0.2 mM EDTA buffer.

If not stated otherwise, all materials were purchased from Sigma-Aldrich, France.

Directly adsorbed intact RBCs

In the case of ATP-free RBCs, cleaned cells were diluted 1:300 (v/v) in SB and incubated for 24h to trigger reversible ATP depletion whereas for ATP-containing RBC, clean erythrocytes were diluted in SB supplemented with 10 mM of D-glucose and incubated for 24h.[24] Finally, a volume of each solution was incubated for 30 min on poly-L-lysine coated mica.

Ghosts from pre-adsorbed RBC

Freshly clean RBC were diluted in SB and incubated for 30 min on poly-L-lysine coated mica. After this incubation period, samples were cleaned ten times with SB to remove excess of unfixed cells. Adsorbed RBC were then incubated 5 min in a low salt buffer (LSB) consisting of 5 mM NaPi (Na_2HPO_4 and NaH_2PO_4) (pH = 7.4), 0.2 mM EDTA and protease inhibitor (Complete Protease inhibitor Cocktail, Roche, France). Then samples were incubated 2 min in a very low salt buffer (vLSB) containing 0.3 mM NaPi (pH = 7.4), 0.2 mM EDTA and protease inhibitor to remove residual hemoglobin. This process was repeated an additional time.

Direct phosphorylation of ghosts was carried out in SB containing 1 mM MgATP.[24] Samples were then incubated during 15 min at room temperature before AFM imaging.

Shear-force opened RBC

Freshly clean RBC were diluted in SB and incubated for 30 min on poly-L-lysine coated mica. Then, samples were cleaned ten times with SB to remove excess of unfixed cells. Adsorbed RBC were then subjected to a stream of 7 mL of SB supplemented with protease inhibitor (Complete

Protease inhibitor Cocktail, Roche, France) at a rate of 0.65 mL/sec with a 21G needle at an angle of 20°. After that samples were incubated twice 2 min in a vLSB to remove residual hemoglobin.[8] To remove spectrin, samples were incubated in vLSB for 60 min at 37°C and then, cleaned ten times in SB.

Direct phosphorylation of ghosts was carried out in SB containing 1 mM MgATP.[24] Samples were then incubated during 40 min at room temperature before AFM imaging.

As a control, Supporting Figure S9 shows the effect of 1 mM $MgCl_2$ and 1 mM MgATP in presence of a casein kinase I inhibitor (Casein Kinase I Inhibitor, D4476. Calbiochem, France) at the extracellular face of ghosts.

PeakForce Quantitative Nano-Mechanics (PF-QNM) AFM measurements

AFM experiments were performed on a multimode-V microscope controlled by Nanoscope-V electronics and the Nanoscope 8 software (Bruker AXS Corporation, Santa Barbara, CA).

Images were acquired in PeakForce Quantitative Nano-Mechanics (PeakForce) mode at different peak loading forces (300 – 500 pN). V-shaped Si_3N_4 cantilevers (MSNL, Bruker AXS Corporation, Santa Barbara, CA) with a nominal spring constant of 0.1 N/m and a nominal tip radius of 3 nm were used under liquid operation. Cantilever spring constant and sensitivity were calibrated before each experiment. The scan speed was 2 Hz, which for a 256 x 256 samples/line image, lead to approx. 2 minutes acquisition time per full topography and nano-mechanics maps. Samples were imaged in salt buffer, except for those cases in which additional treatment was required (e.g. 1 mM MgATP, 1 mM $MgCl_2$, 10 mM D-glucose, and 400 uM CKI inhibitor). PF-QNM images in absence and presence of ATP were performed using the same tip to exclude

experimental variations due to tip size. Data shown is the result of at least triplicates performed in different samples obtained from different days.

AFM image processing

Image and data processing was performed using commercial NanoScope Analysis Software (Bruker AXS Corporation, Santa Barbara, CA) and Gwyddion software, a free modular program for SPM data analysis (gwyddion.net).

Skeleton extraction from AFM topographic images was performed within a Matlab graphical-user-interface environment, available on SI (*gui_network.m*). The skeleton detection from raw AFM images is based on morphomathematical operations. First, a smoothing is performed using a closing operator (*imclose.m function in Matlab*), thus setting the size of the structuring element. Then, the watershed operator detects the contour of the skeleton (*watershed.m function in Matlab*) therefore, giving a suitable tracking of the skeleton pattern at the AFM image [18].

Acknowledgements

This study was supported by the Institut Curie, the Institut National de la Santé et Recherche Médicale (INSERM), the Agence Nationale de la Recherche (ANR), and the City of Paris, and a Fondation Pierre-Gilles de Gennes Fellowship (to LP) and a European Community Marie Curie Intra-European Fellowship for Career Development (to FR). The authors would like to thank Adai Colom Diego to assist with the optical microscopy part, Dr. José Luís Vázquez-Ibar for fruitful discussion and critical reading of the manuscript, and Dr. Timo Betz for scientific discussion.

Author contribution

F.R, L.P and S.S designed the project. L.P performed experiments. F.R and L.P analyzed data. M.D. developed skeleton extraction routine. F.R, L.P and S.S wrote the paper.

Supporting Information Available

Supporting Information includes materials and methods of samples shown in Supporting Figure S1 and details on the Peak Force Quantitative Nanomechanics Imaging and calculations, the characterization of the different samples prepared (Supporting Figure S1), the effect of ATP on the topographic and mechanical remodeling of intact RBCs at different loading forces (300 pN, 400 pN, 500 pN, and retrieved 300 pN) (Supporting Figure S2), profile analysis of images shown in Supporting Figure S2 (Supporting Figure S3), structural insight of the RBC membrane on intact erythrocytes (Supporting Figure S4), the effect of MgATP on the topography and mechanics of the extracellular and cytoplasmic face of RBC membrane at different loading forces (300 pN, 400 pN, 500 pN, and retrieved 300 pN) (Supporting Figure S5 and S7, respectively), an extended version of raw images obtained in these series is displayed in Figure 4 (Supporting Figure S6), a large scan size AFM image acquiered at the cytoplasmic face of RBC membrane (Supporting Figure S8), and a series of images showing the control conditions of the different samples presented (Supporting Figure S9). This material is available free of charge *via* the Internet at http://pubs.acs.org.

References

1. Mohandas, N.; Gallagher, P. G., Red cell membrane: past, present, and future. *Blood* 2008, 112, 3939-3948.

2. Steck, T. L.; Kant, J. A.; Sidney Fleischer, L. P., Preparation of impermeable ghosts and inside-out vesicles from human erythrocyte membranes. In *Methods in Enzymology*, Academic Press: 1974; Vol. Volume 31, pp 172-180.
3. Discher, D. E.; Mohandas, N.; Evans, E. A., Molecular maps of red cell deformation: hidden elasticity and in situ connectivity. *Science* 1994, 266, 1032-1035.
4. Park, Y.; Best, C. A.; Auth, T.; Gov, N. S.; Safran, S. A.; Popescu, G.; Suresh, S.; Feld, M. S., Metabolic remodeling of the human red blood cell membrane. *Proceedings of the National Academy of Sciences* 2010, 107, 1289-1294.
5. Gauthier, E.; Guo, X.; Mohandas, N.; An, X., Phosphorylation-Dependent Perturbations of the 4.1R-Associated Multiprotein Complex of the Erythrocyte Membrane. *Biochemistry* 2011, 50, 4561-4567.
6. Manno, S.; Takakuwa, Y.; Mohandas, N., Modulation of erythrocyte membrane mechanical function by protein 4.1 phosphorylation. *Journal of Biological Chemistry* 2005, 280, 7581-7587.
7. Manno, S.; Takakuwa, Y.; Nagao, K.; Mohandas, N., Modulation of erythrocyte-membrane mechanical function by beta-spectrin phosphorylation and dephosphorylation. *Journal of Biological Chemistry* 1995, 270, 5659-5665.
8. Lange, T.; Jungmann, P.; Haberle, J.; Falk, S.; Duebbers, A.; Bruns, R.; Ebner, A.; Hinterdorfer, P.; Oberleithner, H.; Schillers, H., Reduced number of CFTR molecules in erythrocyte plasma membrane of cystic fibrosis patients. *Mol Membr Biol* 2006, 23, 317-23.
9. Hoppener, C.; Novotny, L., Antenna-based optical imaging of single Ca2+ transmembrane proteins in liquids. *Nano Letters* 2008, 8, 642-646.
10. Kodippili, G. C.; Spector, J.; Sullivan, C.; Kuypers, F. A.; Labotka, R.; Gallagher, P. G.; Ritchie, K.; Low, P. S., Imaging of the diffusion of single band 3 molecules on normal and mutant erythrocytes. *Blood* 2009, 113, 6237-6245.
11. Binnig, G.; Quate, C. F.; Gerber, C., Atomic force microscope. *Phys Rev Lett* 1986, 56, 930-933.
12. Radmacher, M., Studying the mechanics of cellular processes by atomic force microscopy. *Methods Cell Biol* 2007, 83, 347-72.
13. Rico, F.; Su, C.; Scheuring, S., Mechanical Mapping of Single Membrane Proteins at Submolecular Resolution. *Nano Letters* 2011, 11, 3983-3986.
14. Steck, T. L.; Weinstein, R. S.; Straus, J. H.; Wallach, D. F. H., Inside-Out Red Cell Membrane Vesicles: Preparation and Puirification. *Science* 1970, 168, 255-257.
15. Swihart, A. H.; Mikrut, J. M.; Ketterson, J. B.; Macdonald, R. C., Atomic force microscopy of the erythrocyte membrane skeleton. *J Microsc* 2001, 204, 212-25.
16. Le Grimellec, C.; Lesniewska, E.; Cachia, C.; Schreiber, J. P.; Defornel, F.; Goudonnet, J. P., Imaging of the membrane-surface of mdck cells by atomic-force microscopy. *Biophys J.* 1994, 67, 36-41.
17. Li, J.; Lykotrafitis, G.; Dao, M.; Suresh, S., Cytoskeletal dynamics of human erythrocyte. *Proc Natl Acad Sci U S A* 2007, 104, 4937-42.
18. Meyer, F., Topographic Distance And Watershed Lines. *Signal Processing* 1994, 38, 113-125.
19. Veatch, S. L.; Cicuta, P.; Sengupta, P.; Honerkamp-Smith, A.; Holowka, D.; Baird, B., Critical fluctuations in plasma membrane vesicles. *ACS Chem Biol* 2008, 3, 287-93.
20. Betz, T.; Lenz, M.; Joanny, J. F.; Sykes, C., ATP-dependent mechanics of red blood cells. *Proc Natl Acad Sci U S A* 2009, 106, 15320-5.

21. Yoon, Y. Z.; Kotar, J.; Yoon, G.; Cicuta, P., The nonlinear mechanical response of the red blood cell. *Phys Biol* 2008, 5, 036007.
22. Perrotta, S.; del Giudice, E. M.; Iolascon, A.; De Vivo, M.; Di Pinto, D.; Cutillo, S.; Nobili, B., Reversible erythrocyte skeleton destabilization is modulated by beta-spectrin phosphorylation in childhood leukemia. *Leukemia* 2001, 15, 440-4.
23. Lee, J. C.; Discher, D. E., Deformation-enhanced fluctuations in the red cell skeleton with theoretical relations to elasticity, connectivity, and spectrin unfolding. *Biophys J* 2001, 81, 3178-92.
24. Tuvia, S.; Levin, S.; Bitler, A.; Korenstein, R., Mechanical fluctuations of the membrane-skeleton are dependent on F-actin ATPase in human erythrocytes. *Journal of Cell Biology* 1998, 141, 1551-1561.

Figures

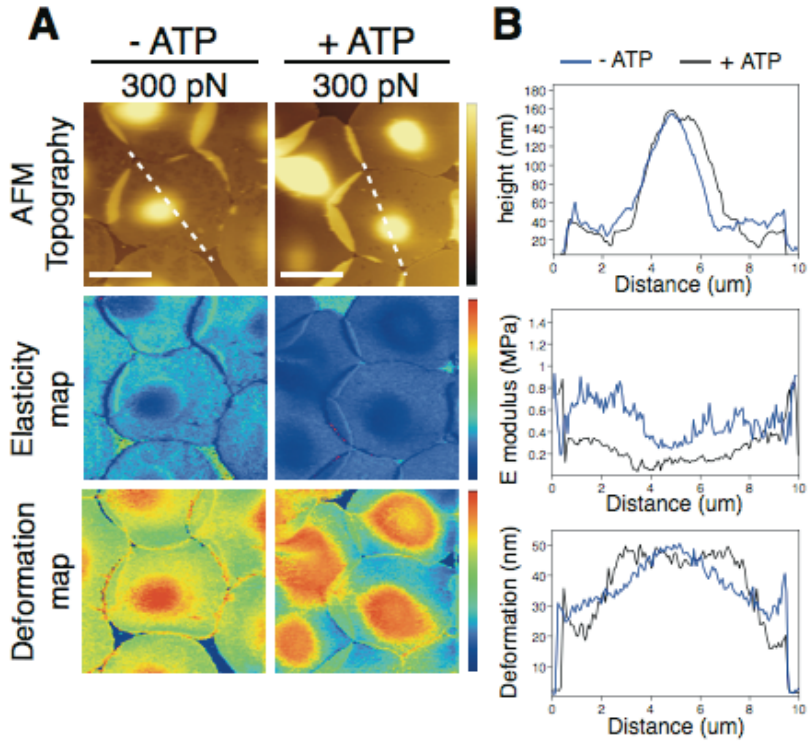

Figure 1. (**A**) Effect of ATP on the topographic and mechanical features (elasticity and deformation map) of intact RBCs directly immobilized on PLL coated mica at 300 pN for ATP-depleted (*left series*) and ATP-containing (*right series*) cells, respectively. (**B**) Profile analysis of topographical images, elasticity and deformation map along the white dashed line for ATP-depleted (*in blue*) and ATP-containing (*in black*) erythrocytes at 300 pN. False color scale is 250 nm for topography, 2.5 MPa for elastic modulus, and 50 nm for deformation. Scale bar is 5 um.

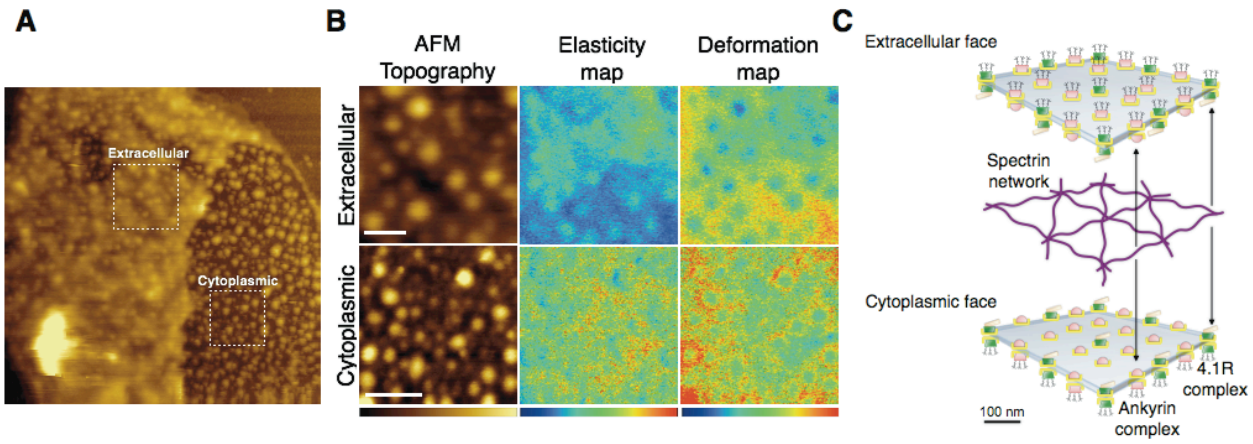

Figure 2. (**A**) AFM topography image displaying an overview of either extracellular or cytoplasmic side of the erytrocyte membrane (*left*). (**B**) Topography, elasticity, and deformation maps of the extracellular (*top*) and cytoplasmic (*bottom*) face of the RBC membrane (*middle series of images*). False color scale is 100 nm for topography, 1.5 MPa for elastic modulus and 50 nm for deformation at extracellular side images, and 20 nm for topography, 6 MPa for elastic modulus and 10 nm for deformation for cytoplasmic side images. Scale bar is 300 nm. (**C**) Scheme of the sub-cellular organization of the erythrocyte membrane (*left*) showing the lattice of macromolecular complexes (4.1R-based in green and ankyrin-based in red) all through the lipid membrane, the spectrin network and the linking points of the spectrin tetramer to both skeleton junctions.

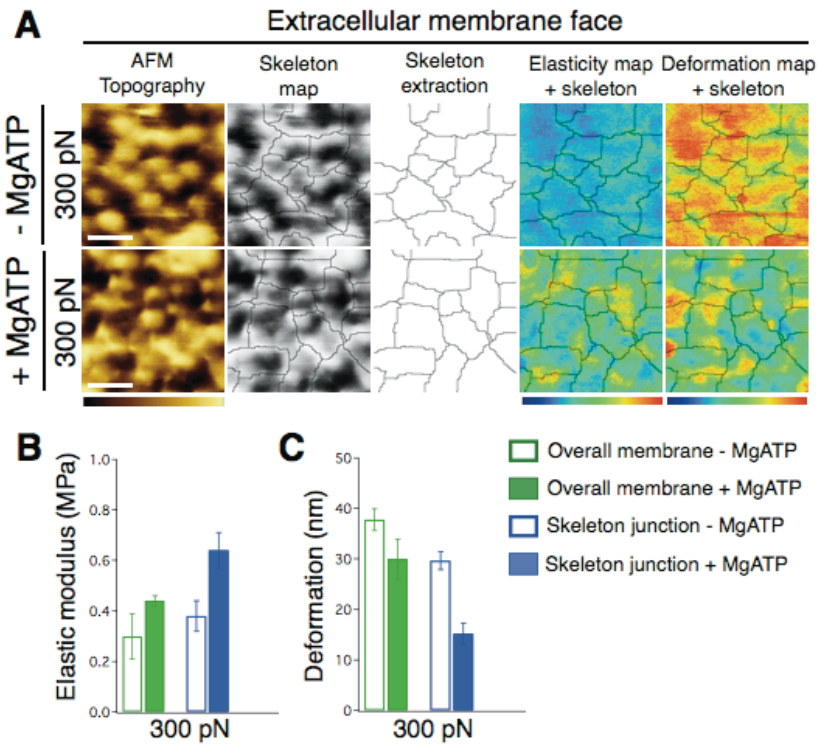

Figure 3. Effect of MgATP on the topography and mechanics of the extracellular face of the RBC membrane. (**A**) AFM maps of topography, elasticity and deformation at 300 pN (without

MgATP, *top series*, and with MgATP *bottom series*). False color scale is 70 nm for topography, 1 MPa for elastic modulus and 30 nm for deformation. Scale bar is 300 nm. (**B**) Elastic modulus (*bottom left*) and **(C)** deformation (*bottom right*) of overall membrane (*green*) and network junctions (*blue*) at 300 pN, both before (*open bars*) and after (*filled bars*) MgATP. Data are shown as mean ± SEM.

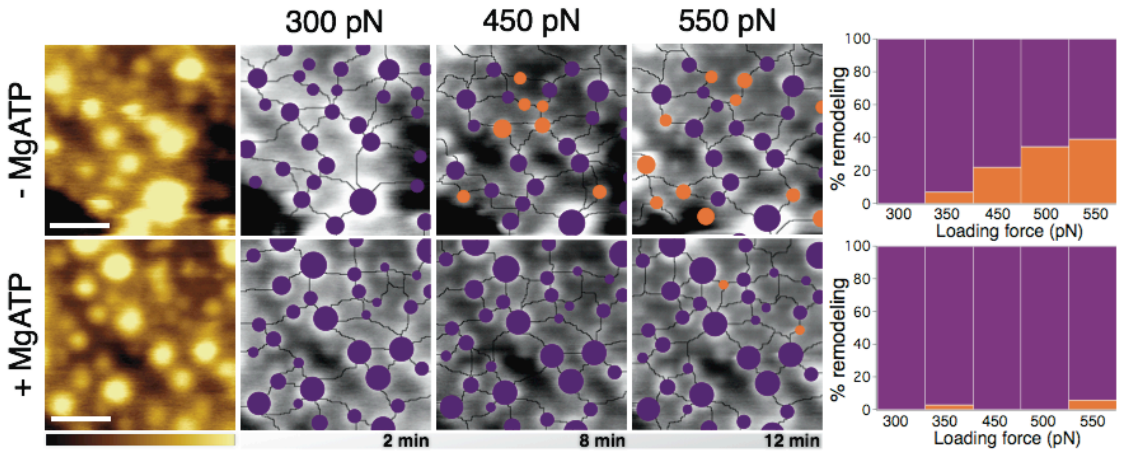

Figure 4. Effect of the loading force and ATP on the topographic remodeling of the RBC extracellular membrane. Topographic AFM images with (*top series*) and without (*bottom series*) MgATP are displayed in a brown color scale (color scale is 70 nm and scale bar is 400 nm). Pictures obtained after skeleton extraction of topographic images at different loading forces (300 pN, 450 pN, and 550 pN) are displayed in grey scale (color scale is 70 nm), showing static junctions (*in purple*) and rearranged junctions (*in orange*). The percentage of extracellular remodeling in presence and absence of ATP is displayed at the end of each series, displaying in orange the % of remodeling (reflecting junction displacements ≥ 50 nm) at each of the loading forces studied (300 pN, 350 pN, 450 pN, 500 pN, and 550 pN). An extended version including the raw images obtained in these series is displayed in Supporting Figure S6.

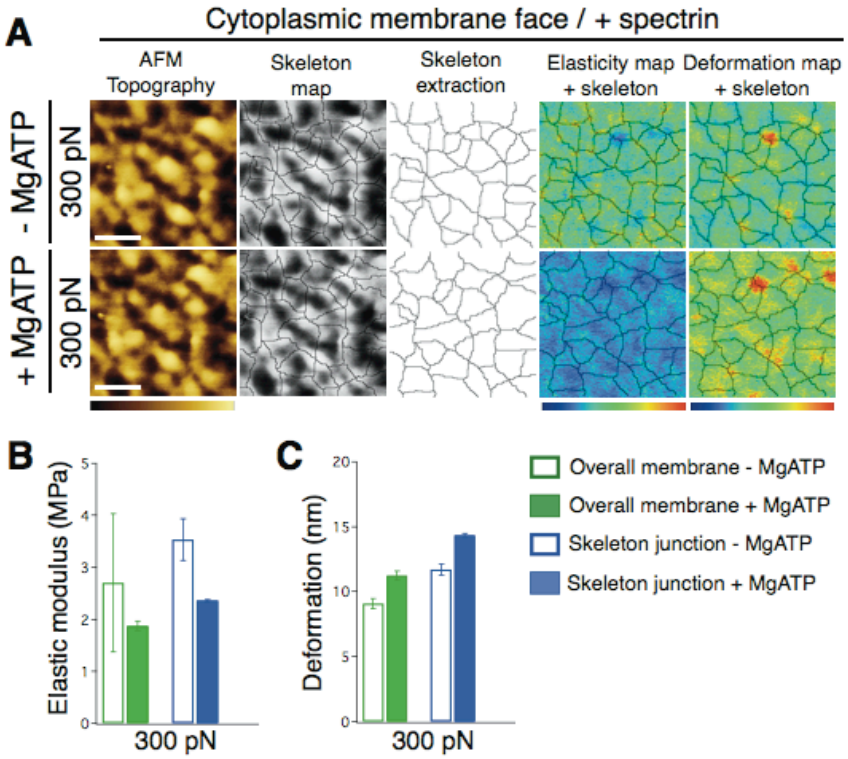

Figure 5. Effect of MgATP on the topography and mechanics of the cytoplasmic face of RBC membrane. (**A**) AFM maps of topography, elasticity and deformation at low loading forces (300 pN) (without MgATP, *top series*, and with MgATP *bottom series*). False color scale is 65 nm for topography, 4 MPa for elastic modulus and 30 nm for deformation. Scale bar is 300 nm. (**B**) Elastic modulus and (**C**) deformation of overall membrane (*green*) and network junctions (*blue*) at 300 pN, before (*open bars*) and after (*filled bars*) MgATP addition. Data are shown as mean ± SEM.

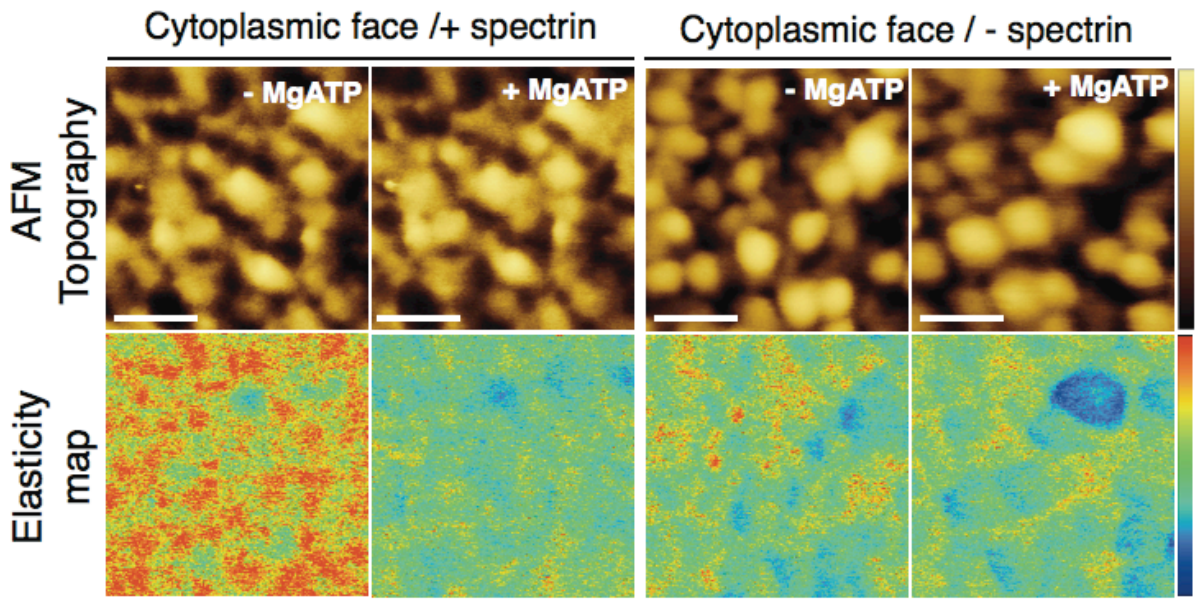

Figure 6. MgATP effect on the topographic (*top*) and elasticity (*bottom*) maps of the RBC cytoplasmic membrane in samples preserving spectrin network (+ spectrin) (*right*) and samples where spectrin network was removed (- spectrin) (*left*). False color scale is 65 nm for topography and 4 MPa for elastic modulus. Scale bar is 300 nm.

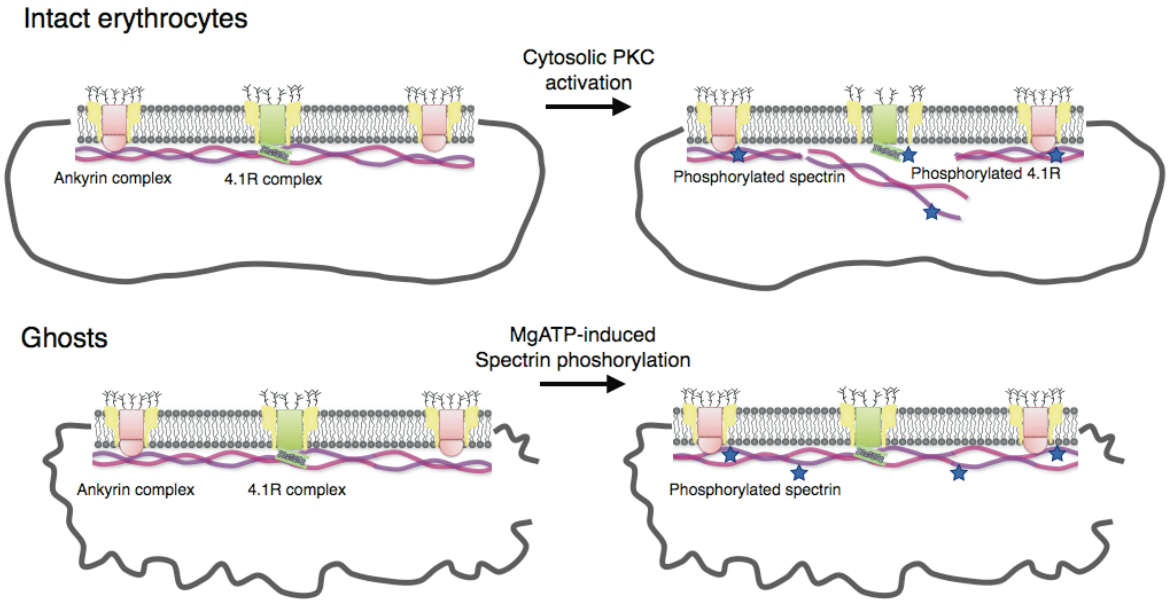

Figure 7. Model explaining the structural and mechanical differences observed at the RBC membrane for intact erythrocytes (*top schematics*) and ghosts (*bottom schematics*). Under normal conditions, membrane stability is fine modulated through several protein phoshporylations including 4.1R, that reversibly releases spectrin after the dissociation of 4.1R complex and glycophorin C, and spectrin, that tightly anchors to the membrane through ankyrin. Therefore, preserved spectrin-membrane connections in ATP depleted cells would explain an increase in membrane tension and elastic modulus. In the case of ghosts, lost of cytosolic kinases triggers selective phosphorylation of spectrin after MgATP addition without any release of spectrin from the 4.1R complex. Spectrin phoshporylation is then materialized in an increase of spectrin-ankyrin affinity and a tight anchor of the sekeleton to the RBC membrane.